

# Damage Mechanisms of Suspended Animal Cells in Agitated Bioreactors with and Without Bubble Entrainment

**Kurt T. Kunas**

*Department of Chemical Engineering, Rice University, P.O. Box 1892, Houston, Texas 77251-1892*

**Eleftherios T. Papoutsakis\***

*Department of Chemical Engineering, Northwestern University, 2145 Sheridan Road, Evanston, Illinois 60208-3120*

*Accepted for publication February 5, 1990*

We show that when freely suspended hybridoma cells are cultured in an agitated bioreactor, two fluid-mechanical mechanisms can cause cell damage and growth retardation. The first is present only when there is a gas phase, and is associated with vortex formation accompanied by bubble entrainment and breakup. In the absence of a vortex and bubble entrainment, cells can be damaged only at very high agitation rates, above approximately 700 rpm, by stresses in the bulk turbulent liquid. Cell damage then correlates with Kolmogorov eddy sizes similar to or smaller than the cell size. In the absence of a vortex, the entrainment and motion of very fine bubbles cause no growth retardation even at agitation rates as high as 600 rpm.

## INTRODUCTION

The number of cell products, whole cells, or cell parts that need to be produced by cell-culture technology is increasing continuously. In fact, more difficult types of cells (such as various fetal cells, malignant cells, hemopoietic and blood cells, and various other human cells) will need to be produced in the future to satisfy the needs for advanced therapies and transplantations, novel diagnostic and testing methodologies, and new therapeutic proteins. Choosing and scaling-up the appropriate bioreactor, depending on the characteristics of the cell, demands that we understand how the complex fluid-mechanical, nutritional, and physico-chemical environment in bioreactors affects the cells.

Growth of anchorage-dependent and freely-suspended animal cells in mixed bioreactors has a variety of advantages such as: scaleability, ease of controlling and monitoring important bioreactor parameters, relatively uniform bioreactor conditions, and use of existing industrial capacity from other biological processes.<sup>1-3</sup> Since animal cells are sensitive to fluid-mechanical forces, an understanding of the damage mechanisms caused by such forces associ-

ated with mixing and/or aeration is important for effective bioreactor design.<sup>4</sup> Oxygen in animal-cell bioreactors is typically supplied by a combination of surface, forced, and/or membrane aeration.

The biomedical-engineering literature contains a wealth of information on how shear stresses affect the morphology, metabolism and product formation of anchorage-dependent and freely-suspended cells associated with the circulatory system, including endothelial cells,<sup>5,6</sup> erythrocytes,<sup>7</sup> platelets,<sup>8</sup> polymorphonuclear leukocytes,<sup>9</sup> and T lymphocytes.<sup>10</sup> These studies have used devices which produce well defined flows and measurable shear stresses on the entire sample volume to characterize the response of cells to various degrees of liquid shear stress. Damage to freely suspended hybridoma cells by shear stresses generated in viscometric flows has also been examined by various researchers.<sup>11-14</sup>

In a mixed bioreactor, cells are exposed not just to simple shear stresses but rather to a complex fluid-mechanical environment generated by turbulence. Croughan and co-workers<sup>15,16</sup> and Cherry and Papoutsakis<sup>17,18</sup> have applied concepts from isotropic turbulence to correlate growth and death rates of anchorage-dependent cells on microcarrier beads with bioreactor parameters. Damage mechanisms of freely suspended cells in agitated bioreactors, with or without surface aeration and/or sparging, have not been systematically examined, and no correlations have been established yet. In an effort to simulate reactor turbulence damage, McQueen and co-workers<sup>19</sup> found that the probability of hybridoma cell lysis during intermittent exposure to turbulent flow in a capillary tube increases with time of exposure and intensity of turbulence. In a number of agitated bioreactors,<sup>3,20-24</sup> and in spinner flasks,<sup>25</sup> cell damage begins at agitation rates anywhere between 150 and 350 rpm. It was recently reported that in bioreactor experiments in which bubble entrainment was carefully avoided, agitation rates up to 450 rpm did not alter hybridoma cell growth.<sup>26</sup>

\* To whom all correspondence should be addressed.

Use of gas sparging (forced aeration) or bubble entrainment, when surface aeration is used, can further complicate the fluid-mechanical environment and cause additional damage to suspension cells.<sup>27–30</sup> Tramper and co-workers<sup>31</sup> have shown that cell damage in a bubble-column reactor may occur at the bubble disengagement at the top of the column or in the area of air injection. Handa et al.<sup>32</sup> presented data to show that cell damage occurs only in the bubble-disengagement region at the top of a bubble column.

Our research aims to investigate and establish the means by which high cell densities of biologically functional cells can be produced efficiently in agitated or mixed bioreactors. Some of the issues that need to be dealt with include the mechanisms of cell damage or metabolic alterations due to fluid-mechanical forces. Understanding of these mechanisms will facilitate the establishment of the agitation and/or sparging limits to which various cells can be exposed. Here we address the problem of cell damage due to agitation and/or bubble entrainment and breakup in the turbulent environment of an agitated bioreactor with and without surface aeration. As a model system to examine this problem, we use a hybridoma cell line (ATCC CRL 8018) which, based on the few available literature data, we have qualitatively judged to be of intermediate shear fragility. This line has been widely used and characterized in our laboratory.<sup>12,22–24</sup>

## MATERIALS AND METHODS

### Cells and Medium

CRL-8018 hybridoma cells (ATCC), which produce an IgM antibody directed against hepatitis B surface antigen, were adapted to grow with 1% Nutridoma-NS or SP (Boehringer, Indianapolis, IN) medium additive and 1% fetal bovine serum (FBS). After adaptation, the cells were routinely cultured in Dulbecco's modified Eagle's medium (DME; Sigma, St. Louis, MO) supplemented with 1% (v/v) FBS (Hyclone Laboratories, Logan, UT), 1% (v/v) Nutridoma-NS or SP, 2 mM glutamine (Sigma), and 50 units/mL penicillin, 0.05 mg/mL streptomycin, and 0.1 mg/mL neomycin (PSN; Sigma) before filtering.

### Bioreactor Cultures

Two Setric Genie 2C bioreactors (Setric Genie Industriel, Toulouse, France) operated with variable (1–2L) working volume were used in all bioreactor experiments. Temperature was controlled at 37°C, and the dissolved oxygen concentration was maintained above 65% saturation with an air/O<sub>2</sub> mixture. The pH was maintained at 7.2 by addition of either CO<sub>2</sub> into the aeration system or 0.5N NaOH to the culture medium. The impeller used for agitation was 7 cm in diameter with four blades pitched at 57° to the horizontal, each blade being 7 by 1.8 cm in dimension. The bioreactors as well as non-agitated T-flasks were inoculated by diluting spinner flask cultures 1:5 to provide an initial cell concentration of 2–2.5 × 10<sup>5</sup> cells/mL. The

bioreactor agitation speed was kept at 60 rpm, a non-damaging speed for the cells, until the cell concentration reached 4–5 × 10<sup>5</sup> cells/mL; then, agitation was increased to the desired rate. Variations in the cell's ability to withstand fluid-mechanical forces due to different inoculum histories, length of lag phase, or culture age<sup>12</sup> were largely overcome by this protocol.

For culture volumes below 2 L, the aeration system within the reactors consisted of a gas headspace in contact with the agitated liquid medium surface. When operated at a volume of 2 L, without a gas headspace, aeration was provided via 3 m of Silastic brand medical grade tubing (Dow Corning, Midland, MI) with 1.47 mm i.d. and 1.97 mm o.d. The tubing was held in place near the vessel wall by a stainless steel wire support.

### Cell Counts and Growth Rates

Total cell concentrations were determined using a coulter counter (Coulter Electronics, Hialeah, FL). Culture viability of random samples was checked using trypan blue dye exclusion in a hemacytometer. The viability was consistently found to be above 95% during exponential growth. Samples were taken every 3–5 h until at least 5 samples within the exponential growth phase had been obtained. The apparent growth rate,  $\mu_{app}$ , was determined by linear regression of the exponential phase of the growth curve, which is a plot of the natural log of the cell concentration versus time. Error bars for the growth rates represent the 95% confidence interval for a regression parameter.<sup>33</sup>

### Vortex and Bubble Characterization

To obtain stationary images of the vortex and bubbles within the reactor, high speed photographs were taken of the reactors containing volumes of 1 or 1.8 L medium at agitation speeds up to 220 rpm using a 35-mm camera and T-MAX P3200 film (Eastman Kodak, Rochester, NY). The approximate size of entrained bubbles could then be estimated from the photographs. In the reactors operated without a gas headspace, a sample was quickly withdrawn from the agitated reactor via a headplate opening using a 5-mL pipet. Bubbles within the sample rose to the surface of the liquid within the pipet and formed a stable foam. The volume of the foam layer as well as the total sample volume could then be measured in the pipet to calculate the percentage of volume occupied by the bubbles. Since the 5-mL pipets used were marked with 0.1-mL increments, the volumes could be measured accurately to approximately ±0.05 mL. To get an estimate of the bubble size, the number of bubbles aligned linearly between divisions of the pipet were counted. The distance between divisions divided by number of bubbles gave a rough estimate of bubble diameter. A more accurate measurement of bubble size was obtained by placing a sample of bubbles from the reactor in a hemacytometer and observing them microscopically. Bubbles in the hemacytometer remained stable for more than 10 min. Since the gap in the hemacy-

tometer was 0.1 mm, only bubbles with diameters less than 0.1 mm could be measured.

## RESULTS

### Cell Growth at Low Agitation Rates in the Presence of a Vortex and Entrained Bubbles

The growth of CRL-8018 hybridoma cells in 1.0 or 1.2 L, surface-aerated bioreactors was evaluated at various agitation rates. The apparent growth rate,  $\mu_{app}$ , was chosen as the primary growth characteristic to be measured. To allow consistent bioreactor behavior from batch to batch, we developed the following protocol. First, healthy, exponentially growing cells were used to provide a consistent inoculum (initial concentration of  $2\text{--}2.5 \times 10^5$  cell/mL) for each run. Second, each reactor culture was allowed to reach the same stage of exponential growth ( $4\text{--}5 \times 10^5$  cells/mL) under conditions of gentle agitation (60 rpm) before the desired agitation level was imposed. Last, after the agitation was increased in each run, at least 5–6 points representing exponential growth were obtained to allow statistically meaningful calculation of the growth rate.

When operated with a volume of 1.0 or 1.2 L, a large vortex was formed around the impeller shaft. The liquid surface at the bottom of this vortex was rapidly fluctuating with bubbles detaching and entraining into the culture medium. From high speed photographs taken of the reactor containing 1.0 L culture medium at agitation rates up to 220 rpm, we observed that the bubbles had an average diameter of 1–3 mm. In addition, the vortex did not come into contact with the blades of the impeller, which means that bubbles detached from the vortex solely as a result of the instability of the gas–liquid interface. No bubble entrainment was observed at agitation rates below 140–150 rpm.

Figure 1 shows the growth rates from batch runs with 1.0 or 1.2 L liquid volume as a function of agitation rate. From Figure 1 the response of hybridoma cells to agitation as well as the effectiveness of the experimental protocol can be assessed. The results from the experiments with the 1 and 1.2 L reactor volumes have been grouped together because the reactor hydrodynamics appear visually similar at these two volumes. The response of the cells in both volumes appears also similar at the agitation rates shown in Figure 1. Up to approximately 190 rpm,  $\mu_{app}$  decreased slowly with increased agitation rate, as shown on the expanded scale for the positive growth rates. At 190–220 rpm,  $\mu_{app}$  dropped dramatically to well below zero. Net positive growth in the 1.0 or 1.2 L reactor does not occur at agitation rates greater than 220 rpm. The large data scatter seen around 200 rpm suggests a delicate balance between cell growth and cell death and/or possibly growth retardation due to fluid-mechanical forces. Above 190–220 rpm, however, cell damage increases much more rapidly than the cells' ability to reproduce, as demonstrated by the large negative  $\mu_{app}$  values. In previous work,<sup>23</sup>  $\mu_{app}$  was modeled as the difference between an invariable "true" growth rate,  $\mu_0$ , and a death rate,  $k$ , that changes in response to differ-

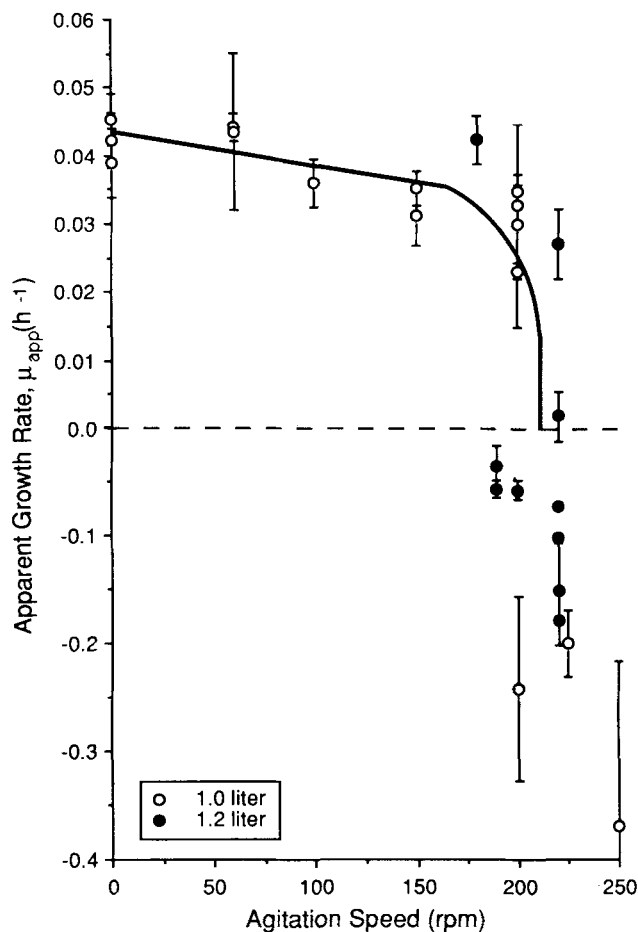


**Figure 1.** Apparent growth rates in agitated bioreactors containing 1.0 or 1.2 L medium at various agitation rates. At the gas–liquid interface and around the impeller shaft a vortex was formed accompanied by bubble entrainment. Growth at zero agitation rate corresponds to T-flask cultures. On the y-axis, the positive and negative values are shown on different scales to emphasize the functional dependency of the positive growth rates on agitation rate. Error bars represent the 95% confidence interval for a regression parameter.

ent agitation rates. Parameter  $\mu_0$  was taken to be constant for simplicity because our data could not discriminate between the two possibilities of a changing versus an invariable  $\mu_0$  with increasing agitation. With this model, the data of Figure 1 can be interpreted to imply that cell death due to fluid-mechanical forces increases very slowly up to approximately 150 rpm, but rapidly above 190–220 rpm.

Typically, error bars have been used in the literature to represent the standard deviation of the mean of several measurements.<sup>6</sup> Here, the error bars represent the 95% confidence level for a regression parameter, and are smaller than the scatter between the data points.

### Cell Growth as a Function of Reactor Volume

One method we used to minimize the vortex and gas entrainment in the reactor was to increase the reactor volume. Increasing the reactor volume reduced the depth of the vortex. As the data of Table I indicate, at both 200 and

**Table I.** Effect of liquid working volume on the growth of hybridoma cells in agitated bioreactors of 2 L total volume. Error estimates represent the 95% confidence interval for a regression parameter.

| Volume (L) | Apparent growth rate (h <sup>-1</sup> ) |
|------------|---|
| 200 rpm:   |   |
| 1.0        | -0.0243 ± 0.0175 <sup>a</sup>           |
| 1.2        | -0.0575 ± 0.0085                        |
| 1.7        | 0.0469 ± 0.0019                         |
| 220 rpm:   |   |
| 1.2        | -0.0795 ± 0.0082 <sup>b</sup>           |
| 1.5        | 0.0280 ± 0.0034                         |
| 1.8        | 0.0424 ± 0.0025                         |

<sup>a</sup> Mean rate from 5 batch runs.

<sup>b</sup> Mean rate from 6 batch runs.

220 rpm, an increase in volume above 1.0–1.2 L did result in a positive rather than negative apparent growth rate. Some values in Table I represent the mean growth rate from several batch runs at the same volume and agitation speed. The error interval for a mean growth rate reported in Table I is the square root of the sum of the squares of the error intervals for each individual growth rate used to calculate the mean, divided by the number of growth rates used to calculate the mean. As expected, high speed photographs of the reactors revealed a smaller vortex in reactors containing 1.8 L medium than in the reactors with only 1.0 L medium.

### Cell Growth in the Absence of a Gas Headspace but in the Presence Small Entrained Bubbles

In order to investigate if cell damage is due to fluid forces in the bulk of the liquid phase, or to stresses resulting from vortex instabilities and the associated bubble entrainment, we modified the reactors to operate without a gas headspace. In the modified system the volume was increased to 2 L, which completely filled the reactor and brought the fluid level in contact with the reactor headplate. Without any gas headspace, a vortex could not form regardless of the agitation rate. For oxygenation and pH control, each reactor was equipped with 6 m of thin-walled silicone tubing wrapped around a stainless steel support cage. Because the support cage held the tubing within 1 cm of the reactor wall, the fluid region around the impeller remained unimpeded.

While the filled reactors eliminated the formation of a vortex, as samples were periodically removed from an opening in the headplate, small amounts of air were introduced into the reactors. At the high agitation speeds used in the filled reactors, any air within the reactor was quickly entrained into the liquid to form very small bubbles. As the run progressed, and more samples were taken, the concentration of bubbles within the reactor increased. During a typical run the bubbles accounted for approximately 1–3% of the fluid volume and ranged in size from approximately 300 to 50  $\mu\text{m}$  in diameter. Using these values, the

concentration of bubbles in the reactor was calculated to be on the order of 5000 bubbles/mL. Under such conditions, the medium in the agitated reactor has the appearance of a whitish emulsion which is typical of high-agitation microbial fermentations.

Figure 2 shows the results of experiments using the filled reactors in which many fine bubbles were formed. To find the range of agitation rates which would result in slower apparent cell growth, the agitation rate was increased several times during each batch run. After an increase in agitation, 2 or 3 points were taken to determine if the cell concentration was increasing or decreasing. The agitation rate was then increased again. Thus, several agitation conditions could be tested during each batch run, although the measurement of the growth rate at each agitation rate was somewhat less accurate. However, accurate growth rate measurements were obtained at select agitation rates using additional experiments at a single speed. As Figure 2 shows, even in the presence of small bubbles entrained in the liquid, good net cell growth was observed at agitation rates up to 700 rpm. In Figures 2(a) and 2(b), the cells continued exponential growth at apparent rates of  $0.0511 \pm 0.0042 \text{ h}^{-1}$  up to 450 rpm and  $0.0417 \pm 0.0035 \text{ h}^{-1}$  up to 600 rpm. These growth rates were calculated using points from several agitation speeds, since the increases in agitation speeds did not affect the apparent exponential growth of the cells. The apparent growth rates at 600 and 400 rpm were statistically indistinguishable, and, in fact, no different from the rates under mild agitation conditions (Fig. 1). We conclude that up to 600 rpm, in the absence of a vortex and a gas phase, but even in the presence of very fast moving small bubbles, agitation is not detrimental to cell growth. The apparent growth rates of cells at 800 and 900 rpm were calculated from data taken at a single speed only as shown in Figures 2(c) and 2(d) and were found to be  $0.0015 \pm 0.0047 \text{ h}^{-1}$  and  $-0.0187 \pm 0.0084 \text{ h}^{-1}$ , respectively. In all runs [Figs. 2(a)–2(d) and 3], a large jump in cell concentration occurred immediately following the initial increase in agitation from the gentle rate of 60 rpm. We found that cells grow loosely attached in the interstices between the rows of silicone tubing and are dislodged and become suspended at the onset of higher agitation rates.

### Cell Growth in the Absence of a Gas Headspace and Entrained Bubbles

In further experiments we again modified the reactors to completely eliminate vortex formation and bubble entrainment and isolate the damaging effects of bulk-liquid fluid forces from those associated with bubble entrainment, motion, and breakup. In addition to completely filling the reactor, a sampling device was connected which allowed culture medium to be withdrawn from the reactor without opening a port on the headplate. A reservoir was attached so that fresh medium could flow into the reactor as sample medium was removed. This reactor system, which also included aeration via silicone tubing, successfully eliminated

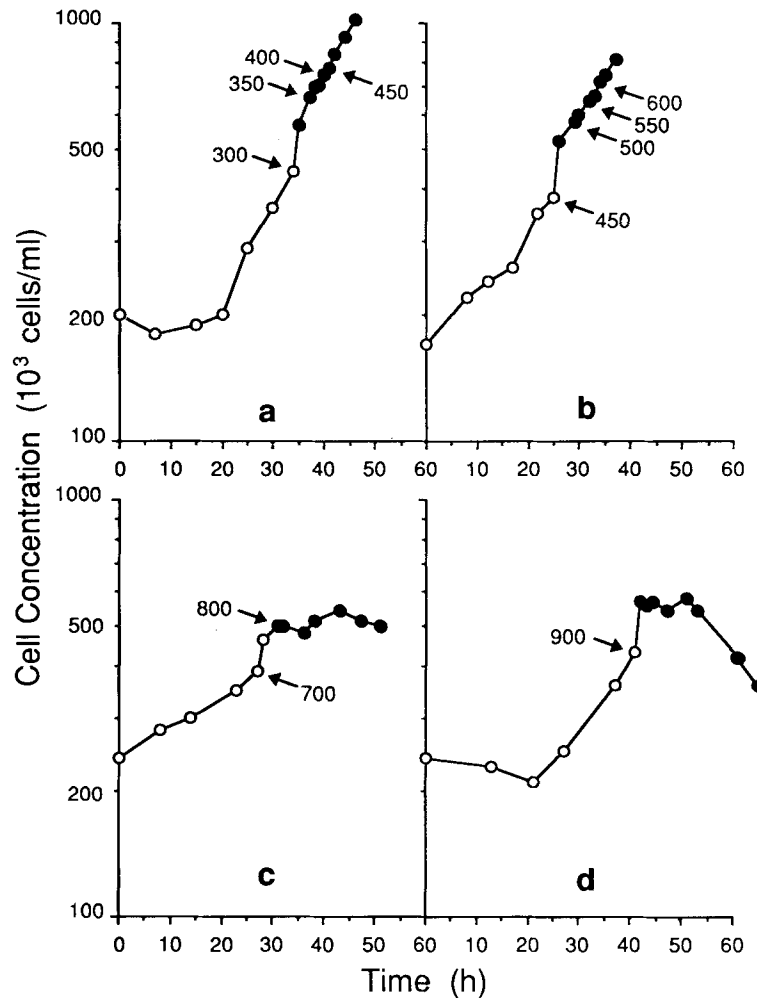


**Figure 2.** Batch growth curves for hybridoma cultures grown in the 2 L agitated bioreactor without a gas headspace. Oxygenation and pH control was accomplished via silicone tubing. Cultures were stirred at an agitation rate of 60 rpm until a cell concentration of  $4\text{--}5 \times 10^5$  cells/mL was obtained. The agitation was increased to the given values at the points indicated by the arrows. During the course of each run, large amounts of bubbles ranging in size from 50 to 300  $\mu\text{m}$  were entrained into the culture medium, although a vortex was absent. The filled symbols represent the points of exponential cell growth used to calculate apparent growth rates of (a)  $0.0511 \pm 0.0042 \text{ h}^{-1}$ , (b)  $0.0417 \pm 0.0035 \text{ h}^{-1}$ , (c)  $0.0015 \pm 0.0047 \text{ h}^{-1}$ , and (d)  $-0.0187 \pm 0.0084 \text{ h}^{-1}$ . The error estimates represent the 95% confidence limit for a regression parameter.

bubble entrainment in the reactor, even at an agitation speed of 800 rpm.

Figure 3 shows the results of a batch reactor run at 800 rpm in which no bubbles were present in the reactor medium. The cells grew with an apparent growth rate of  $0.0155 \pm 0.0055 \text{ h}^{-1}$  compared to the much lower rate of  $0.0015 \pm 0.0047 \text{ h}^{-1}$  obtained in the presence of entrained bubbles at 800 rpm [Fig. 2(c)]. The growth rate at 800 rpm was significantly lower than typical growth rates under conditions of no agitation or gentle agitation (an average of  $0.045 \text{ h}^{-1}$ ). This suggests that, at agitation rates above approximately 600 rpm, some cell damage is due to stresses within the bulk turbulent liquid phase in addition to stresses associated with the motion, coalescence and breakup of

gas bubbles within the liquid. The results of Figure 3 demonstrate that cells can grow at agitation speeds up to at least 800 rpm, as long as a vortex and bubble entrainment can be eliminated. Such agitation rates are more typical of microbial bioreactors and have not been previously accomplished in cell culture reactors. Although of possibly little practical significance, it is not unlikely that, at larger scales and with different impeller design, cell growth at even higher agitation rates may be feasible.

Cell damage in turbulent microcarrier bioreactors has been associated and correlated with the relative size of Kolmogorov-scale turbulent eddies to the microcarrier size.<sup>15-18</sup> Cell damage due to direct interaction between the cells on the microcarriers and the surrounding fluid or due

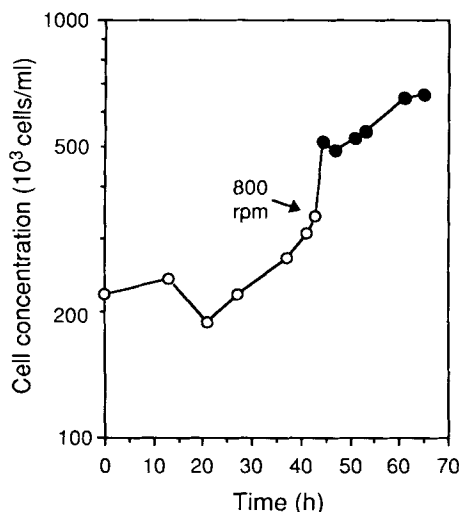


**Figure 3.** Batch growth curve for hybridoma cells growing in the 2 L agitated bioreactor without a gas headspace and without the presence of entrained bubbles. Agitation was increased from 60 to 800 rpm at the point indicated by the arrow. The points represented by the filled symbols were used to calculate an apparent growth rate of  $0.0155 \pm 0.0055 \text{ h}^{-1}$ . The error estimate represents the 95% confidence limit for a regression parameter.

to bead to bead interactions becomes severe when the Kolmogorov-scale eddy size,  $\eta$ , becomes similar to or smaller than the microcarrier size.<sup>15-18</sup> Damage to freely suspended cells during intermittent turbulent flow through a capillary tube has been shown to occur when the Kolmogorov-scale eddies are similar in size to the cell size.<sup>19</sup> An analogous possibility for freely suspended cells has not been examined in agitated reactors, since, up to now, cell damage in agitated reactors was observed at agitation rates below 300–450 rpm, whereby  $\eta$  is still considerably larger than the free cell size (10–15  $\mu\text{m}$  diameter). As we have shown here, at these lower agitation rates, agitation damage is due to bubble entrainment and breakup, and that only at rates above approximately 600–700 rpm does cell damage due to fluid forces in the absence of bubbles become important. This is the only case where the eddy-size correlation might be valid.  $\eta$  is calculated from the equation<sup>15-18</sup>:

$$\eta = (\nu^3/\epsilon)^{1/4} \quad (1)$$

where  $\nu$  is the kinematic viscosity and  $\epsilon$  is the specific turbulent power dissipation rate:

$$\epsilon = N_p n^3 d_i^5 / V_d \quad (2)$$

$d_i$  is the impeller diameter (here 7 cm);  $N_p$  is the dimensionless power number;  $n$  is the agitation rate in rev/s; and  $V_d$  is the power dissipation volume. However, several ambiguities exist when calculating the eddy size in a stirred bioreactor. First, the volume in which energy is dissipated may be taken as the entire reactor volume or merely the volume in the vicinity of the impeller, roughly the impeller diameter cubed; the latter is a better choice.<sup>17</sup> Second, the impellers used in our reactors are not standard marine pro-

pellers or flat-bladed, Rushton turbines, thus making the estimation of an impeller power number from existing correlations somewhat ambiguous. Using a reasonable range of power numbers and both the total reactor volume and volume in the vicinity of the impeller,  $d_i^3$ , the Kolmogorov-scale eddy size for the completely filled bioreactor at an agitation rate of 800 rpm is tabulated in Table II. One may therefore conclude that, indeed, when the eddy size becomes similar to the cell size, cell damage due to fluid forces occurs even in the absence of a gas phase.

## DISCUSSION

In the 1.0 and 1.2 L reactors at 190–220 rpm, bubbles rapidly detach from the bottom of a fluctuating vortex, are entrained, swirl throughout the liquid volume, then rise and disengage at the liquid surface. These conditions result in a rapid decline in cell concentration as a result of irreparable cell damage. By increasing the reactor volume and decreasing the size of the vortex, cell damage can be controlled even at very high agitation rates. For the volume increases used in the present work, it is not valid to argue that the reduced cell damage may be attributed to a larger volume available for energy dissipation; i.e. to a lower  $\epsilon$  and thus larger  $\eta$  [eqs. (1) and (2)]. This is because  $\epsilon$  is inversely proportional to  $V_d$  while it increases with the third power of the agitation rate,  $n$ . Thus, even if one assumes that the agitation power is dissipated in the entire liquid volume,  $V_d$  increases only by 67–100% (from 1–1.2 to 2 L), while  $n$  increases by at least 300% (from 200 to 600–700 rpm) without observing significant cell damage. Indeed, in the completely filled reactors, cell growth was observed at agitation rates up to 700 rpm, even in the presence of very small bubbles.

Thus, our results show that cell damage in an agitated bioreactor, at rates above approximately 150 rpm, is associated with the presence of a gas–liquid interface within the reactor. In the absence of a vortex, the presence of a gas–liquid interface in the form of entrained bubbles down to 50  $\mu\text{m}$  in size does not necessarily cause cell damage,

**Table II.** Range of eddy sizes calculated for a single agitation rate of 800 rpm for the completely filled reactor (2000  $\text{cm}^3$ ) depending upon the value used for the power number and the volume available for power dissipation,  $V_d$ , in the reactor.

| Power number                     | Kolmogorov eddy size ( $\mu\text{m}$ ) |
|----------------------------------|--|
| $V_d = 2000 \text{ cm}^3$        |  |
| 1.5                              | 22.2                                   |
| 2.0                              | 20.7                                   |
| 2.5                              | 19.6                                   |
| $V_d = d_i^3 = 343 \text{ cm}^3$ |  |
| 1.5                              | 14.3                                   |
| 2.0                              | 13.3                                   |
| 2.5                              | 12.6                                   |

Note: Parameter  $d_i$  is the impeller diameter (cm).

as it was observed at agitation rates below 600 rpm. Only when entrained bubbles interact with a freely moving gas-liquid interface, such as that present between the culture medium and gas headspace, does significant cell damage occur. Unlike what is often tacitly assumed, neither the small size nor the large concentration of bubbles appear by themselves detrimental to cells. Indeed, under the present conditions, the rapidly moving (with respect to a stationary frame of reference), very small bubbles (50–300  $\mu\text{m}$ ) cause no reduction of cell growth at agitation rates up to at least 600 rpm. On the contrary, at lower agitation rates (150 rpm and higher), much fewer, much larger (1–3 mm), slower moving bubbles cause a large amount of cell damage when a gas phase is present. This is a useful observation of potentially practical significance because it may imply that, with proper reactor design, direct sparging at high agitation rates may be feasible without causing cell damage. What design would make this feasible is not yet clear because we have no quantitative understanding, or any possible correlations, of how bubble entrainment and breakup damage cells.

At 800 rpm, which corresponds to a Kolmogorov eddy size comparable to the cell size of 12–15  $\mu\text{m}$ , cells grow at a very low apparent growth rate when large amounts of small bubbles are entrained in the reactor liquid. In the absence of any entrained gas, growth at 800 rpm is positive but slower than growth under gentle agitation conditions. Therefore, at agitation rates above 600–700 rpm, some damage to cells can be attributed to stresses from the turbulent liquid even in the absence of a gas phase. In the presence of large numbers of small, entrained bubbles, and at agitation rates above 600–700 rpm, both mechanisms apparently contribute to cell damage. As with other systems of suspended cell “particles”, which include 150–180  $\mu\text{m}$  microcarrier beads, 80  $\mu\text{m}$  protozoa cells,<sup>15–18,34</sup> and the present 12–15  $\mu\text{m}$  cells, cell damage due to interactions in the turbulent bulk liquid correlates with a Kolmogorov eddy size,  $\eta$ , similar to the “particle” size. Although the ratio of  $\eta$  to the cell size may be used as a predictor of cell damage, it provides no details as to how cells are damaged by their interaction with these eddies, or even a proof that there is indeed a direct cell to eddy interaction.

We have presented some of the data from Figure 1 in an earlier article<sup>24</sup> as a function of the Kolmogorov-scale shear stress,  $\tau = \rho(\epsilon\nu)^{1/2}$ , that corresponds to the eddy size  $\eta$ . Since no foam formation and no gas entrainment was visible with the naked eye, we had thought that cell damage was due to stresses within the bulk liquid alone. We argued then that since the eddy size  $\eta$  was much larger than the cells, damage was the result of stresses within these eddies. However, as the later experiments reported here show, the Kolmogorov-scale eddies and the associated shear stresses resulting from agitation in the range shown in Figure 1 were not the cause of cell damage. Interestingly, the correlation with  $\tau$  is still valid, but we have no explanation for it.

Handa et al.<sup>30</sup> reported that cell damage in a bubble column reactor is caused in the area of bubble disengagement

at the surface of the reactor. They proposed two possible damage mechanisms—rapid oscillations due to bursting bubbles and shear forces in draining films in foams. For insect cells grown in a bubble column, Tramper and Vlak<sup>27,31</sup> suggested that cell damage may occur at the area of injection or surface disengagement of the bubble. They also suggested that shear forces caused by rising bubbles are not a cause of cell damage. These mechanism of cell damage in bubble-column reactors are consistent with our findings that cell damage at agitation rates above 150 rpm (but below 600–700 rpm) occurs only when bubbles are bursting at the liquid surface. In addition, cells do grow in the presence of suspended bubbles that do not disengage at an interface, even at high agitation rates (up to 700 rpm).

This research was supported in part by the U.S. National Science Foundation under grant EET-8896100 and matching grants from the Monsanto Corporation and the Eastman-Kodak Company.

## References

1. J. R. Birch, K. Lambert, P. W. Thompson, A. C. Kenney, and L. A. Wood, “Antibody Production with Airlift Fermentors,” in *Large Scale Cell Culture Technology*, B. K. Lydersen, Ed., (Hanser, Munich, 1987), pp. 1–20.
2. J. D. Macmillan, D. Velez, L. Miller, and S. Reuveny, “Monoclonal Antibody Production in Stirred Reactors,” in *Large Scale Cell Culture Technology*, B. K. Lydersen, Ed., (Hanser, Munich, 1987), pp. 21–58.
3. M. P. Backer, L. S. Metzger, P. L. Slaber, K. L. Nevitt, and G. B. Boder, *Biotechnol. Bioeng.*, **32**, 993 (1988).
4. R. Bliem, *Trends Biotechnol.*, **7**, 197 (1989).
5. J. A. Frangos, S. G. Eskin, L. V. McIntire, and C. L. Ives, *Science*, **227**, 1477 (1985).
6. S. L. Diamond, S. G. Eskin, and L. V. McIntire, *Science*, **243**, 1483 (1989).
7. E. A. O’Rear, M. M. Udden, L. V. McIntire, and E. C. Lynch, *Biochim. Biophys. Acta*, **691**, 274 (1982).
8. J. D. Hellums and R. A. Hardwick, “Response of Platelets to Shear Stress—a Review,” in *The Rheology of Blood, Blood Vessels and Associated Tissues*, D. R. Gross and N. D. C. Hwang, Eds., (Sijthoff and Noordhoff, Rockville, MD, 1981), pp. 160–183.
9. B. G. Rhee, E. R. Hall, and L. V. McIntire, *Blood*, **267**, 240 (1986).
10. K. K. Chittur, L. V. McIntire, and R. R. Rich, *Biotechnol. Prog.*, **4**, 89 (1988).
11. I. Abu-Reesh and F. Kargi, *J. Biotechnol.*, **9**, 167 (1989).
12. J. F. Petersen, L. V. McIntire, and E. T. Papoutsakis, *J. Biotechnol.*, **7**, 229 (1988).
13. U. Schuerch, H. Kramer, A. Einsele, F. Widmer, and H. M. Eppenberger, *J. Biotechnol.*, **7**, 179 (1988).
14. C. G. Smith, P. F. Greenfield, and D. H. Randerson, “Shear Sensitivity of Three Hybridoma Cell Lines in Suspension Culture,” in *Modern Approaches to Animal Cell Technology*, R. E. Spier and J. B. Griffith, Eds., (Butterworths, London, 1987), pp. 316–327.
15. M. S. Croughan, J.-F. Hamel, and D. I. C. Wang, *Biotechnol. Bioeng.*, **29**, 130 (1987).
16. M. S. Croughan, J.-F. Hamel, and D. I. C. Wang, *Biotechnol. Bioeng.*, **32**, 975 (1988).
17. R. S. Cherry and E. T. Papoutsakis, *Biotechnol. Bioeng.*, **32**, 1001 (1988).
18. R. S. Cherry and E. T. Papoutsakis, *Bioproc. Eng.*, **4**, 81 (1989).
19. A. McQueen, E. Meilhoc, and J. E. Bailey, *Biotechnol. Lett.*, **9**, 831 (1987).
20. F. de St. Groth, *J. Immunol. Methods*, **57**, 121 (1983).
21. T. C. Dodge and W. S. Hu, *Biotechnol. Lett.*, **8**, 683 (1986).
22. K. T. Kunas and E. T. Papoutsakis, *J. Biotechnol.*, to appear.
23. K. T. Kunas and E. T. Papoutsakis, *Biotechnol. Lett.*, **11**, 525 (1989).

24. E. T. Papoutsakis and K. T. Kunas, "Hydrodynamic Effects on Cultured Hybridoma Cells CRL 8018 in an Agitated Bioreactor," in *Advances in Animal Cell Biology and Technology for Bioprocesses, Proceedings of the 9th Meeting of the European Society for Animal Cell Technology*, R. E. Spier et al., Eds., (Butterworths, London, 1989), pp. 203–211.
25. G. M. Lee, T. K. Huard, M. S. Kaminski, and B. O. Palsson, *Biotechnol. Lett.*, **10**, 625 (1988).
26. M. Al-Rubeai, A. N. Emery, and A. W. Nienow, "The Effect of Agitation on Growth and Antibody Production of Hybridoma Cells—Preliminary Results," in *Advances in Animal Cell Biology and Technology for Bioprocesses, Proceedings of the 9th Meeting of the European Society for Animal Cell Technology*, R. E. Spier et al., Eds., (Butterworths, London, 1989), pp. 221–223.
27. J. Tramper, J. B. Williams, and D. Joustra, *Enzyme Microb. Technol.*, **8**, 33 (1986).
28. D. W. Murhammer and C. F. Goochee, *Bio/Technology*, **6**, 1411 (1988).
29. B. Maiorella, D. Inlow, A. Shauger, and D. Harano, *Bio/Technology*, **6**, 1406 (1988).
30. A. Handa, A. N. Emery, and R. E. Spier, *Dev. Biol. Standard.*, **66**, 241 (1987).
31. J. Tramper, D. Smit, J. Straatman, and J. M. Vlak, *Bioprocess Eng.*, **3**, 37 (1988).
32. A. Handa-Corrigan, A. N. Emery, and R. E. Spier, *Enzyme Microb. Technol.*, **11**, 230 (1989).
33. B. L. Bowerman, R. T. O'Connell, and D. A. Dickey, *Linear Statistical Models—An Applied Approach*, (Duxbury Press, Boston, 1986).
34. M. Midler, Jr. and R. K. Finn, *Biotechnol. Bioeng.*, **8**, 71 (1966).